



**Landslide susceptibility assessment based on different machine-learning  
methods in Zhaoping County of eastern Guangxi**

Chunfang Kong<sup>1,2,3,4</sup>, Kai Xu<sup>1,2,3,\*</sup>, Junzuo Wang<sup>1</sup>, Chonglong Wu<sup>1,2,3</sup>, Gang Liu<sup>1,2</sup>

<sup>1</sup>School of Computer, China University of Geosciences, Wuhan, 430074, China

<sup>2</sup>Hubei Key Laboratory of Intelligent Geo-Information Processing, Wuhan, 430074, China

<sup>3</sup>Innovation Center of Mineral Resources Exploration Engineering Technology in Bedrock Area,  
Ministry of Natural Resources, Guiyang, 550081, China

<sup>4</sup>National-Local Joint Engineering Laboratory on Digital Preservation and Innovative  
Technologies for the Culture of Traditional Villages and Towns, Hengyang, 421000, China

Corresponding author: Kai Xu

E-mail address: [xukai@cug.edu.cn](mailto:xukai@cug.edu.cn)

Phone: +862767883286, +8615327232692

Mobile: +862767883051



14 **Abstract:** Regarding the ever increasing and frequent occurrence of serious landslide disaster in  
15 eastern Guangxi, the current study were implemented to adopt support vector machines (SVM),  
16 particle swarm optimization support vector machines (PSO-SVM), random forest (RF), and  
17 particle swarm optimization random forest (PSO-RF) methods to assess landslide susceptibility by  
18 Zhaoping County. To this end, 10 landslide disaster-related causal variables including digital  
19 elevation model (DEM)-derived, meteorology-derived, Landsat8-derived, geology-derived, and  
20 human activities factors were selected for running four machine-learning (ML) methods, and  
21 landslide susceptibility evaluation maps were produced. Then, receiver operating characteristics  
22 (ROC) curves, and field investigation were performed to verify the efficiency of these models.  
23 Analysis and comparison of the results denoted that all four ML models performed well for the  
24 landslide susceptibility evaluation as indicated by the values of ROC curves -- from 0.863 to 0.934.  
25 Moreover, the results also indicated that the PSO algorithm has a good effect on SVM and FR  
26 models. In addition, such a result also revealed that the PSO-RF and PSO-SVM models have the  
27 strong robustness and stable performance, and those two models are promising methods that could  
28 be transferred to other regions for landslide susceptibility evaluation.

29 **Keywords:** Landslide; Susceptibility evaluation; Machine-learning (ML); Particle swarm  
30 optimization (PSO); Support Vector Machines (SVM); Random Forest (RF)



## 31 **1. Introduction**

32 The geological environment in eastern Guangxi is fragile and landslide disaster occur  
 33 frequently, which not only causes huge economic losses and ecological damage, but also seriously  
 34 restricts the survival of human beings and the sustainable development of human society  
 35 (Pourghasemi et al., 2012; Huang and Zhao, 2018; Chen et al., 2019). With the rapid development  
 36 of the economy in recent decades, the frequency and intensity of landslide disaster are rapidly  
 37 increasing with the over-exploitation and utilization of natural resources by humans (Zhang et al.,  
 38 2016). Therefore, it is of great significance to objectively evaluate the landslide susceptibility for  
 39 the reduction and prevention of the disasters.

40 In recent years, more and more machine-learning (ML) algorithms have been optimized and  
 41 applied for landslide susceptibility assessment in different regions. Examples are: Bayesian  
 42 network (BN) (Song et al., 2012; Pham et al., 2016), Naïve Bayes (NB) (Tien Bui et al., 2012;  
 43 Pham et al. 2015, 2016), artificial neural networks (ANN) (Choi et al., 2012; Zare et al., 2013;  
 44 Conforti et al., 2014; Pham et al. 2015; Xu et al., 2015; Tien Bui et al., 2016; Aditian et al., 2018;  
 45 Zhou et al., 2018), Support Vector Machines (SVM) (Marjanović et al., 2011; Tien Bui et al.,  
 46 2012; 2016; Pourghasemi et al., 2013; Pradhan, 2013; San, 2014; Kavzoglu et al., 2014; Peng et  
 47 al., 2014; Hong et al. 2015; Pham et al., 2016; Kumar et al., 2017; Ada and San, 2018; Zhou et al.,  
 48 2018; Aktas and San, 2019; Wang et al., 2019; Zhang et al., 2019), Logistic Regression (LR)  
 49 (Choi et al., 2012; Kavzoglu et al., 2014; Hong et al. 2015; Trigila et al., 2015; Pham et al., 2016;  
 50 Tien Bui et al., 2016; Lin et al., 2017; Sevgen et al., 2019; Wang et al., 2019), decision tree (DT)  
 51 (Tien Bui et al., 2012; Pradhan, 2013; Tsai et al., 2013; Youssef et al., 2016; Hong et al., 2018;



52 Khosravi et al., 2018; Aktas and San, 2019), Random Forest (RF) (Trigila et al., 2015; Youssef et  
 53 al., 2016; Chen et al., 2017; Ada and San, 2018; Aktas and San, 2019), Fisher's linear  
 54 discriminant analysis (FLDA) (Rossi et al., 2010; Murillo-García and Alcántara-Ayala, 2015),  
 55 SVM-ANN (Xia et al., 2018), SVM-LR (Wang et al., 2019), convolutional neural network  
 56 (CNN)-SVM, CNN-RF and CNN-LR (Fang et al., 2020). These have all been used to  
 57 quantitatively predict and assess the susceptibility for landslide in different regions of the world.  
 58 These studies play an important role in the susceptibility evaluation and prediction of landslide.

59 In addition, many comparative studies on landslide susceptibility assessment using different  
 60 ML methods have been performed. For example, Marjanović et al. (2011) stated a comparison  
 61 research of SVM with other models and found that SVM has the best performances compared with  
 62 DT and LR for landslide susceptibility evaluation. In another landslide assessment investigation,  
 63 Tien Bui et al. (2012) also proved that the capability of SVM was better than the decision tree and  
 64 NB models. Another comparative investigation, Trigila et al. (2015) completed a comparison of the  
 65 LR and RF algorithms in an analytic study of landslide susceptibility and discovered that RF  
 66 presents a better performance than LR. Another comparative study on performance of landslide  
 67 susceptibility mapping, Kavzoglu et al. (2014) made an experimental research to investigate that  
 68 the performance of SVM is higher than the LR. Another study certified that results produced from  
 69 SVM have the highest prediction accuracy compared to LR, BN, NB, and FLDA for landslide  
 70 susceptibility evaluation (Pham et al., 2016). Likewise, another comparative research on the  
 71 performance of two ML algorithms, SVM and FR, for landslide susceptibility prediction based on  
 72 two-level random sampling, was compared by Ada and San (2018).



73           In general, each of the above ML models has been widely applied to landslide prediction and  
74   evaluation. Among them, SVM and RF have been widely proved to be useful methods in the  
75   evaluation of landslide susceptibility (Marjanović et al., 2011; Tien Bui et al., 2012; Kavzoglu et  
76   al., 2014; Trigila et al., 2015; Pham et al., 2016; Ada and San, 2018). However, few studies have  
77   focused on the optimization of SVM and RF models in landslide susceptibility prediction and  
78   evaluation and compared the optimized results. Therefore, the objective of the present paper is to:  
79   (1) determine the landslide susceptibility assessment factors by multi-source data fusion and  
80   correlation factor analysis; (2) optimize SVM and RF models by using a particle swarm  
81   optimization (PSO) algorithm; (3) analyze and evaluate the susceptibility levels of landslide by  
82   using the SVM, PSO-SVM, RF, and PSO-RF models for Zhaoping County; and (4) compare the  
83   performances of four ML models for landslide susceptibility evaluation by receiver operating  
84   characteristic (ROC) curve, statistic analysis, and field-verified methods. The results provide  
85   valuable informational support for the prediction and evaluation of landslide in Zhaoping County,  
86   Guangxi.



## 2. Study areas and materials

### 2.1. Study areas

Zhaoping County is located between longitude  $110^{\circ}34'E$  to  $111^{\circ}19'E$  and latitude  $23^{\circ}39'N$  to  $24^{\circ}24'N$  in the eastern part of Guangxi, the middle reaches of the Guijiang River, with a total area of about  $3,223.67\text{km}^2$  and a total population of 448,000, as shown in Fig. 1. It is situated in the subtropical monsoon humid climate region with mild climate and abundant rainfall. The annual average temperature is  $19.8^{\circ}\text{C}$  and the annual rainfall is 2046 mm, which is one of the rainy and heavy rain centers in Guangxi.

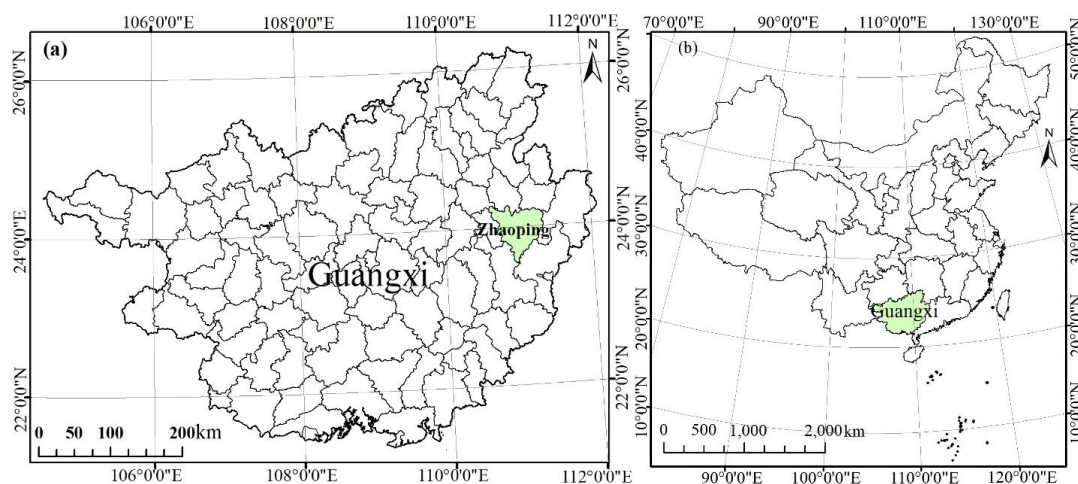


**Fig. 1.** Location of Zhaoping County in Guangxi Province (a) and China (b)

Zhaoping County has remarkable geomorphological characteristics; it is in a mountainous region with intervening deep valleys, where the mountain area is 87.6% of the total area, and the terrain is high in the northwest and low in the southeast. The main structure is near EN to WS trending large fault and north protruding Dayaoshan arc structural compression belt, where a



101 series of secondary arc folds and faults are distributed. At the same time, the Dayaoshan uplift  
102 belt is cut by a series of near-SN trending faults and it forms many secondary depression areas.  
103 Under the influence of multi-stage tectonic movements, joint fissure is developed in rock mass  
104 and rock is weathered seriously, which provides the basic conditions for the formation of  
105 landslide. Finally, extremely fragile geological characteristics are formed, because of long-term  
106 geological changes in geological internal and external forces; these landslide occurred frequently  
107 in Zhaoping County. According to the detailed survey data of landslide in 2018 in the Guangxi  
108 Geological Survey Bureau, there are 345 hidden danger points of landslide in Zhaoping County.

## 109 **2.2. Data sources and hazards inventory data**

110 Following are the main data sources adopted in this paper: (1) A digital elevation model  
111 (DEM) for Zhaoping County with a spatial resolution of 30m×30m; it was constructed from  
112 ASTER Global DEM acquired from the United States Geological Survey  
113 (<http://earthexplorer.usgs.gov>). Based on the DEM data, three geomorphic factors were generated:  
114 slope, aspect, and plan curvature. (2) The annual precipitation data was collected from the  
115 government of Guangxi Meteorological Bureau; (3) Landsat 8 OLI image (2017/12/24, 124/043)  
116 used to extract the normalized differential vegetation index (NDVI), and land use and land cover  
117 (LULC) map; (4) 1:50 000 topographic map was collected to reflect the densities of residents and  
118 road network. (5) 1:50 000 geological map was adopted to extract the stratum lithology and  
119 tectonic complexity. (6) A landslide inventory map in Zhaoping County was prepared from field  
120 investigation of Guangxi Geological Survey Bureau.



### 2.3. Classification of evaluation factors

There are many kinds of factors affecting the occurrence of landslide in Zhaoping County, and the factors are not independent of each other. To more objectively assess the susceptibility of landslide, a total of ten hazards affecting factors were chosen based on the results of field investigation of Guangxi Geological Survey Bureau and the characteristics of landslide distribution in Zhaoping County; they are slope, aspect, curvature, annual rainfall, NDVI, stratum lithology, tectonic complexity, LULC, residential density, and road network density. At the same time, these factors have been classified into different grades (Table 1) according to the analysis of influence of each evaluation factor to landslide occurrences implemented by Guangxi Geological Survey Bureau for Zhaoping County.

**Table 1** Landslide affecting factors and their classes

No.	Evaluation factor	Classification
(a)	Slope (°)	1-[0,7); 2-[7,13); 3-[13,19); 4-[19,25); 5-[25,34); 6-[34,50); 7-[50,70); 8-[70,76)
(b)	Aspect (°)	1-[0,22.5); 2-[22.5,67.5); 3-[67.5,112.5); 4-[112.5,157.5); 5-[157.5,202.5); 6-[202.5,247.5); 7-[247.5,292.5); 8-[292.5,360)
(c)	Plan curvature	1-[-25,-5); 2-[-5,-2.5); 3-[-2.5,-1); 4-[-1,0); 5-[0,1); 6-[1,2.5); 7-[2.5,5); 8-[5,28.9)
(d)	Annual rainfall (mm)	1-[0,1980); 2-[1980,2100); 3-[2100,2220); 4-[2220,2340); 5-[2340,2460); 6-[2460,2580); 7-[2580,2700); 8-[2700,2820)
(e)	NDVI	1-[0,0.01); 2-[0.01,0.09); 3-[0.09,0.17); 4-[0.17,0.25); 5-[0.25,0.33); 6-[0.33,0.4); 7-[0.4,0.5); 8-[0.5,0.71)
(f)	Stratum lithology	0-River; 1-Quaternary; 2-carbonate rock; 5-clasolite intercalated with siliceous rocks; 6-clastic rock; 7-sandstone and shale; 8-granite or basal rocks
(g)	Tectonic complexity	1-[0,1.4); 2-[1.4,2.7); 3-[2.7,3.8); 4-[3.8,4.9); 5-[4.9,6); 6-[6,7.3); 7-[7.3,8.9); 8-[8.9,9.4)
(h)	LULC	1-cultivated land; 2-woodland; 3-grassland; 4-river and lake; 5-construction land
(i)	Residential density	1-[0,1.2); 2-[1.2,2.7); 3-[2.7,4.5); 4-[4.5,6.9); 5-[6.9,10.1); 6-[10.1,14.2); 7-[14.2,19.7); 8-[19.7,25)
(j)	Road network density (km/km <sup>2</sup> )	1-[0,3.2); 2-[3.2,4.7); 3-[4.7,6.1); 4-[6.1,7.8); 5-[7.8,9.7); 6-[9.7,11.7); 7-[11.7,13.9); 8-[13.9,14)

According to the classification standard of Table 1, the attribute value of each evaluation





factor is obtained by superimposed analysis with a 30m\*30m grid and the attributes of each evaluation factor; the results are shown in Fig. 2(a-j). Thereinto, Fig. 2(a-c) indicates that maps of slope (Fig. 2a), aspect (Fig. 2b), and curvature (Fig. 2c) were extracted from DEM with a 30m\*30m grid cell, which represented the influence of topography on the development and distribution of landslide in Zhaoping County.

Precipitation, especially heavy rain or continuous precipitation is the external dynamic factor that induces landslide (Zhang et al., 2016). There is plenty of precipitation in Zhaoping County, and the annual average number of heavy rain days is between 3 and 15 days. Under the action of precipitation infiltration, scour, erosion, and so on, unstable mountains easily form landslide. Meanwhile, the landslide and frequent periods of heavy rain are basically the same, both concentrated from May to August, indicating that the formation of landslide is closely related to heavy rain in Zhaoping County. Figure 2d is the annual rainfall map of Zhaoping County from the Guangxi Meteorological Bureau.

The ecological environment is closely related to the occurrence of landslide. Zhaoping County has a warm and humid climate with a wide variety of vegetation. In this current study, the map of NDVI (Fig. 2e) was extracted from a Landsat8 OLI image to characterize the ecological environmental characteristics for Zhaoping County.

The strata of Zhaoping County are mainly Cambrian, Devonian, and a small number of Quaternary, and the main lithology are clastic rocks, clastic rocks intercalated with siliceous rocks, sandstone and shale, carbonate rock, and a small amount of granite or basal rock, accounting for 55.89%, 34.11%, 4.54%, 3.96%, and 0.47% of the total area, respectively (Fig. 2f).

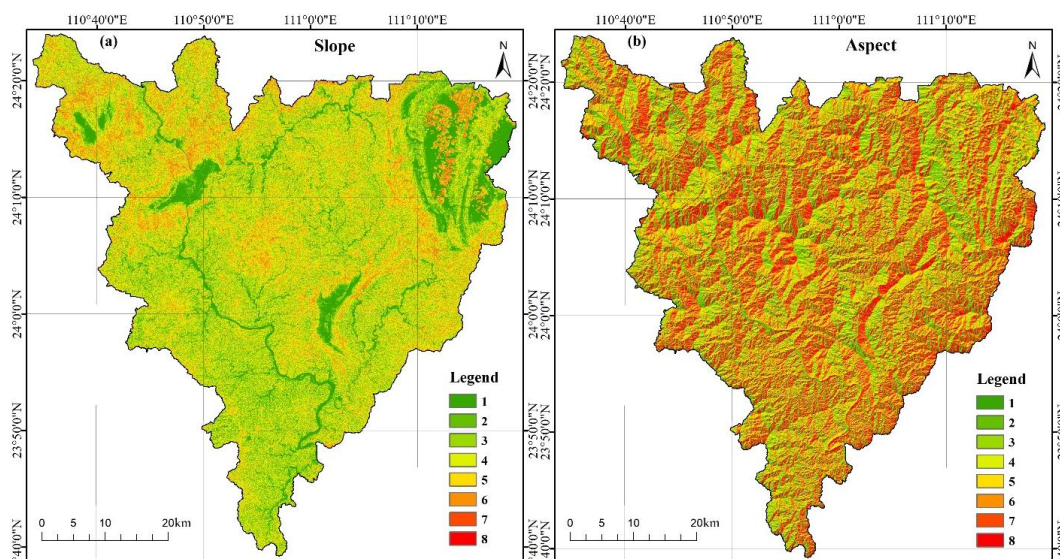


154   Clastic rocks are prone to landslides under the action of precipitation, especially heavy  
155   precipitation (Zhang et al., 2016). At the same time, after the influence of multi-stage tectonic  
156   movement and long-term action of geological internal and external forces, a more complex  
157   geological structure pattern is formed, and folds and fractures staggered distribution, which  
158   resulted in extremely fragile geological environmental characteristics in Zhaoping County. Figure  
159   2g indicates the tectonic complexity of Zhaoping County.

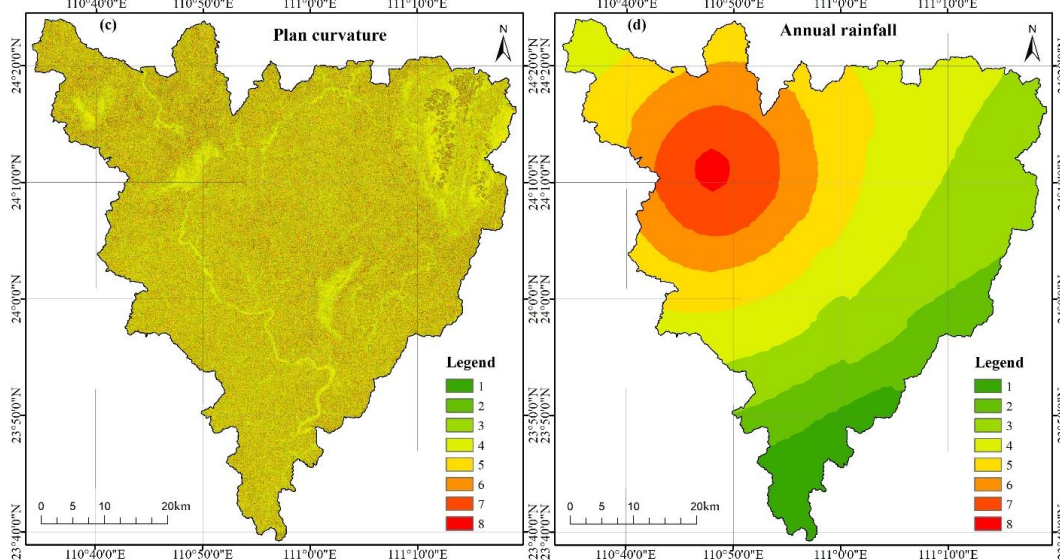
160       In addition, human activities have become one of the major driving forces for environmental  
161   changes and induced landslide (Zhang et al., 2016). Human engineering activities such as land  
162   use change, steep slope reclamation, road and bridge building, development of forests and  
163   mineral resources, construction of hydropower engineering and so on, strongly disturb the  
164   topography and geomorphology and make it lose its equilibrium state, which leads to the  
165   probability of landslide occurring far more than in the natural state. Therefore, LULC map,  
166   residential density, and road network density were selected as representative factors to reflect the  
167   influences of human activities on the environment in Zhaoping County, as shown in Fig. 2(h-j).



168

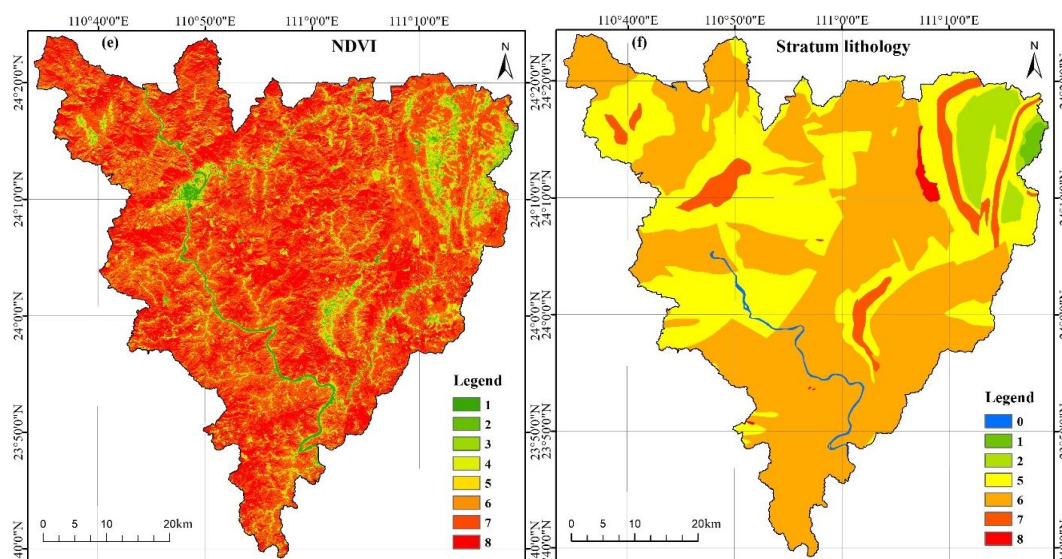


169

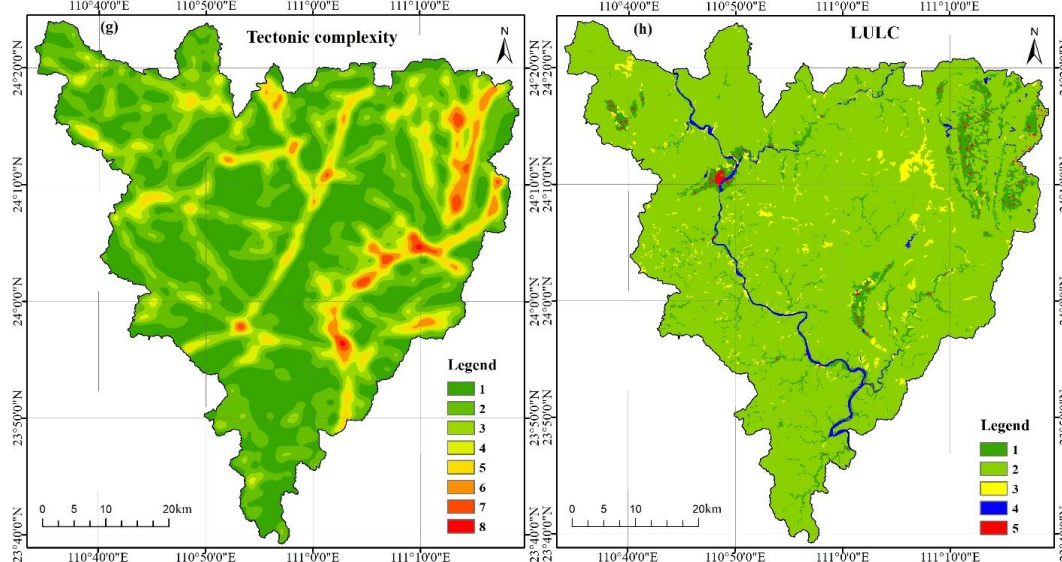




170



171





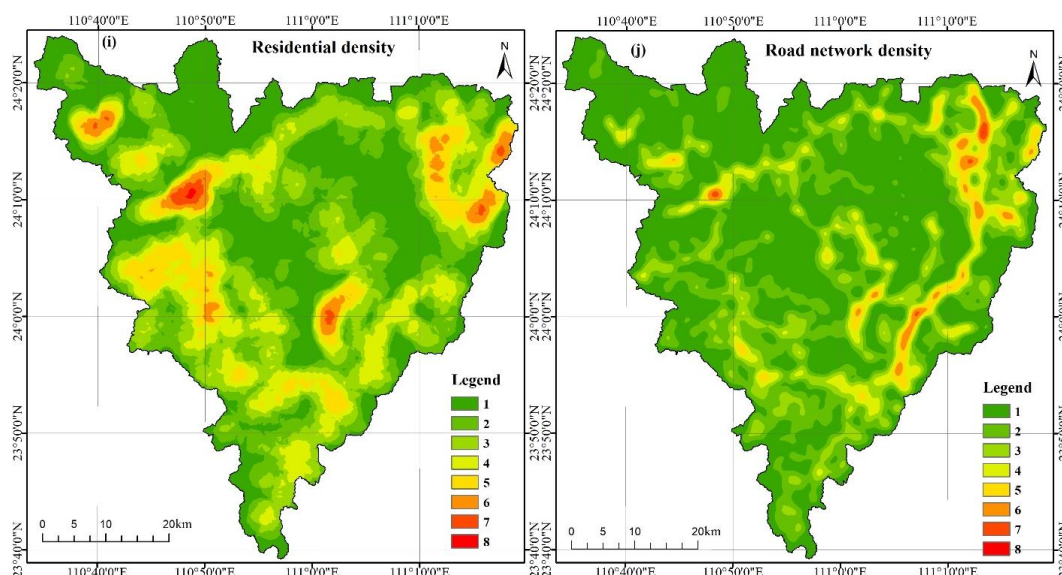


**Fig. 2.** Attribute value of landslide evaluation factors [(a) slope, (b) Aspect, (c) Plan curvature, (d) Annual rainfall, (e) NDVI, (f) Stratum lithology, (g) Tectonic complexity, (h) LULC, (i) Residential density, (j) Road network density]

On the basis of the above, the database of the landslide susceptibility evaluation factors in Zhaoping County was established, with a total of 3,581,859 grid evaluation units. In the present database, 1,493 grid units as training samples were selected to construct the training dataset, including 242 landslide hazards points and 1,251 non-hazards points; 1,042 grid units as testing samples to construct the testing dataset, including 103 landslide hazards points and 939 non-hazards points. Four ML models (SVM、PSO-SVM、RF and PSO-RF) for geological hazard susceptibility evaluation were trained using the training dataset, whereas the performance of the constructed four landslide susceptibility evaluation models was verified using the testing dataset.



### 184 3. Methods

185 Landslide susceptibility evaluation has been carried out in nine main processes (Fig. 3): (1)  
 186 According to the environmental characteristics of Zhaoping County, all the evaluation factors  
 187 related to landslide are collected; (2) Evaluation units were divided into 30m×30m grid cells by  
 188 using ArcGIS; (3) The landslide susceptibility assessment factor system was determined; (4)  
 189 Classification criterion for each evaluation factor was divided according to the classification  
 190 standard of Guangxi Geological Survey Bureau; (5) Spatial and attribute databases for each  
 191 evaluation factor were set up based on 30m\*30m grid cells; (6) Training and testing datasets were  
 192 selected; (7) Landslide susceptibility evaluation models were established based on different ML  
 193 methods, such as SVM, PSO-SVM, RF, and PSO-RF; (8) We validated and compared the  
 194 evaluation accuracy for four ML models with ROC curves, statistical analysis, and field-survey;  
 195 And (9) we divided the landslide susceptibility levels in Zhaoping County.

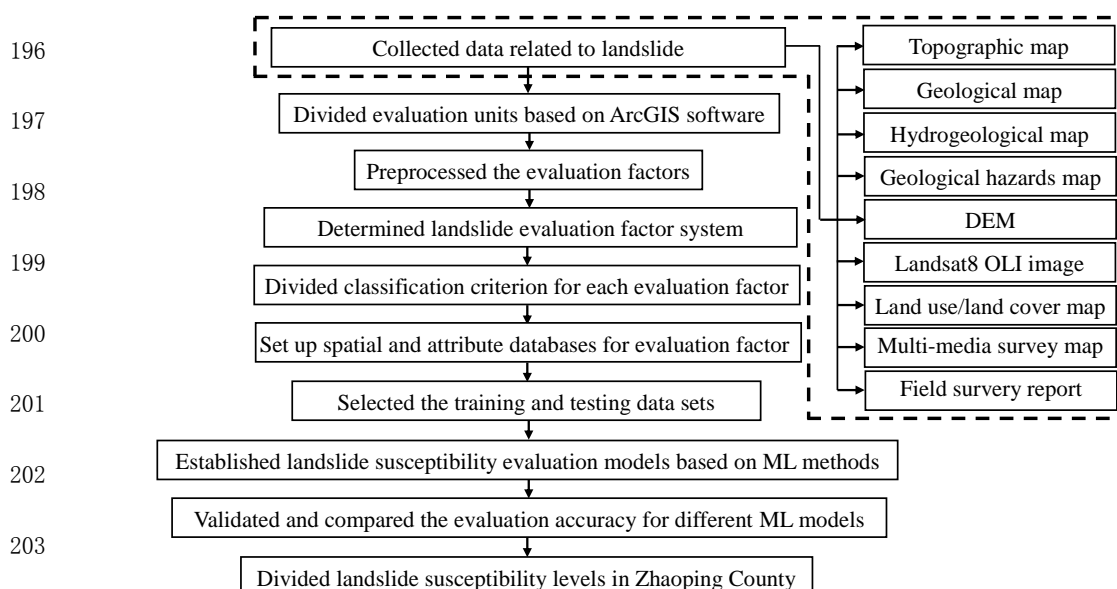


**Fig. 3.** Flowchart of landslide susceptibility evaluation based on ML



### 204 3.1. SVM model

205 Support vector machine (SVM) is based on statistical approach and structured risk  
 206 minimization theory (Cortes and Vapnik, 1995; Vapnik, 1995). It uses kernel function to map the  
 207 input variables to a high-dimensional characteristic space, and then finds the optimal hyperplane  
 208 for separating two classes. The SVM ensures that the extreme solution is the global optimal  
 209 solution (Kavzoglu et al., 2014). At present, SVM has been proven to have many unique  
 210 advantages in dealing with small samples, nonlinear and high-dimensional pattern recognition, and  
 211 is successfully applied in hazards prediction and assessment ( Marjanović et al., 2011; Tien Bui et  
 212 al., 2012; Pradhan, 2013; Kavzoglu et al., 2014; Pham et al., 2016; Ada and San, 2018).

213 In the landslide assessment of the current study, the training sample set is given as  $\{x_i, y_i\}, i =$   
 214  $1, 2, \dots, n; x_i \in R^m, y_i \in \{-1, +1\}$ . SVM seeks the optimal classification superplane in the  
 215 feature space of the landslide, which can separate the two types of training samples of the hazards  
 216 point and the non-hazards point. The optimal classification superplane is defined as the following:

$$217 \quad \begin{aligned} & \min_{w,b} \frac{1}{2} \|w\|^2 \\ & \text{s. t. } y_i(w^T x_i + b) \geq 1, i = 1, 2, \dots, m \end{aligned} \quad (1)$$

218 where  $n$  represents the number of training samples,  $m$  represents the dimension of the input  
 219 vector,  $\|w\|$  represents the norm of the superplane normal vector, and  $b$  is the displacement term.

220 The Lagrangian multiplier rule is introduced to find the extreme value, and the auxiliary  
 221 function is generated as follows:

$$222 \quad L(w, b, \lambda) = \frac{1}{2} \|w\|^2 - \sum_{i=1}^m \lambda_i (y_i(w^T x_i + b) - 1) \quad (2)$$

223 where the  $\lambda_i$  is Lagrange multiplier.



224 The dual minimum method given by Vapnik (1995) and Tax and Duin (1999) is used to solve  
 225 the  $w$  and  $b$  values of the equation.

226 For the nonlinear non-separable hazards samples, the non-negative relaxation variables ( $\xi_i$ )  
 227 and penalty factor  $C$  are introduced to adjust the constraint conditions, and the formula is modified  
 228 to:

$$\begin{aligned} \min_{w,b} \quad & \frac{1}{2} \|w\|^2 + C \sum_{i=1}^m \xi_i \\ \text{s. t. } & y_i(w^T x_i + b) \geq 1 - \xi_i, i = 1, 2, \dots, m \end{aligned} \quad (3)$$

230 where  $\xi_i > 0$  denotes a sample classification error;  $C$  represents the degree of the penalty. In the  
 231 landslide assessment,  $C \in (0,1]$  denotes that the support vector represents the percentage of the  
 232 entire training set. Therefore, the smaller the value of  $C \sum_{i=1}^n \xi_i$ , the better for finding the  
 233 classification hyperplane.

234 Meanwhile, the radial basis kernel function  $k(x, x_i)$  is adopted to process the nonlinear  
 235 decision boundary when the SVM is constructed based on the training sample set. As shown in the  
 236 formula (4):

$$k(x, x_i) = \exp\left(-\frac{\|x - x_i\|^2}{2\sigma^2}\right) \quad (4)$$

238 where  $\sigma^2$  represents the kernel parameter, which implicitly decides the distribution of data after  
 239 mapping to a new characteristic space. The number of support vectors affects the speed of  
 240 training and prediction.

241 To bring the kernel function into (3), the final regression function (the optimal hyperplane) is  
 242 obtained as formula (5):

$$g(x) = \sum_{i=1}^n \lambda_i y_i k(x_i, x) + b \quad (5)$$





244 The evaluation results of landslide susceptibility in Zhaoping County are obtained by using  
 245 regression analysis of formula (5) and parameter optimization. Furthermore, the natural breakpoint  
 246 method is adopted to divide the susceptibility into five levels: extremely high, high, middle, low,  
 247 and extremely low areas (Fig. 4a).

### 248 3.2. SVM model based on particle swarm optimization (PSO-SVM)

249 From the above analysis, it can be seen that the selection of the SVM parameters (penalty  
 250 factor  $C$ , and the core parameter of radial basis function  $\sigma$ ) directly affects the prediction  
 251 accuracy of the landslide susceptibility evaluation model (Kavzoglu et al., 2014). Therefore, the  
 252 particle swarm optimization (PSO) algorithm with powerful parameter global search capability  
 253 was adopted to select the optimal  $C$  and  $\sigma$ , and the PSO-SVM model for prediction and evaluation  
 254 of landslide was set up in Zhaoping County. The main steps of the PSO-SVM model can be  
 255 summed up as Table 2:

256 **Table 2** The main steps of the PSO-SVM model

<b>(1) Initialization:</b>
The initial parameters of the PSO-SVM model are set, including species size, iteration times, learning factor, inertia weight, initial particle and particle initial velocity. The particle vector represents a SVM model corresponding to different $C$ and $\sigma$ .
<b>(2) Optimization:</b>
In the process of particle optimization, each solution of the optimization problem is called a particle in the search space. The particle adaptation value ( $f_i$ ) is calculated according to the fitness function. Adaptive function is the measure basis of the selection individual, and the individual is evaluated by the fitness function.
<b>(3) Replacement:</b>
On the basis of the objective function, the adaptive value of each particle ( $f_i$ ), the population individual optimal solution $f_i(p_{best})$ , and the population global optimal solution $f_i(p_{gbest})$ were calculated and compared. If $f_i < f_i(p_{best})$ , then the optimization solution of the previous round is replaced with the new adaptation value ( $f_i$ ), and the particles of the previous round is replaced with the new particles, and then the $f_i(p_{best})$ of each particle is compared with the $f_i(p_{gbest})$ of all particles. If $f_i(p_{best}) < f_i(p_{gbest})$ , the optimal solution of each particle is used to replace the optimal solution of all the original particles, and the current state of the particles is saved at the same



time.

#### (4) Determination:

If the  $f_i$  of the individual in the population meets the requirements, or if the evolutionary algebra is terminated, then the calculation is ended, and the particle individual corresponds to the optimal  $C$  and  $\sigma$  combination, otherwise go to step (2) to continue the iteration.

#### (5) Set up the PSO-SVM model:

The global optimal PSO-SVM model is obtained by using the optimal parameters of the SVM with the optimal  $C$  and  $\sigma$  combination to train the training samples. The susceptibility of landslide is quantitatively evaluated and divided into five levels: extremely high, high, middle, low, and extremely low areas (Fig. 4b).

### 257 3.3. Random Forests (RF) model

258 Random Forests (RF) is a cluster tree classification proposed by Breiman (2001), which is  
 259 composed of several unrelated decision trees. It is put back from the original training dataset by  
 260 the Bagging algorithm to obtain multi-Bootstrap training data sets. And then the corresponding  
 261 decision tree model was acquired by training random selection of  $m$  attributes from all  $M$  decision  
 262 attributes. Finally, the final classification result of the test set samples was determined by voting.

263 Suppose that for the landslide sample  $x$  of Zhaoping County, the output of the  $g$  decision tree  
 264 is  $f_{tree,g}(x) = i, i = 1, 2, \dots, n$ , that is, its corresponding category,  $g = 1, 2, \dots, G$ ,  $G$  is the  
 265 number of decision trees in RF, then the output of the RF model is as follows:

$$266 \quad f_{RF}(x) = \arg \max_{i=1,2,\dots,n} \{G(f_{tree,g}(x) = i)\} \quad (6)$$

267 where  $G(\cdot)$  represents the number of samples that satisfy the expressions in parentheses.

268 The construction process of the RF model for landslide susceptibility assessment in  
 269 Zhaoping County is as Table 3:

270 **Table 3** The main steps of the RF model

#### (1) Initialization:



Suppose  $D$  is an original training data set of landslide susceptibility assessment factors, which is composed of  $M$  prediction attributes ( $M=10$ ) and a classification attribute  $Y$  ( $Y=5$ ). There is  $n$  ( $n=3,581,859$  different examples in  $D$ ).

#### (2) Get multiple training datasets:

The  $K$  new training subsets of  $\{D_1, D_2, \dots, D_K\}$  were obtained by  $K$  times random sampling with replay from the original training data set  $D$  by using Bagging algorithm. At the same time, each of the  $K$  training subsets contains  $n$  instances, in which there is repetition.

#### (3) Training to generate decision tree:

For each training subset  $D_i$  ( $1 \leq i \leq K$ ), the decision tree without pruning is generated by the following procedure:

Firstly, let the number of predictive attributes in the training sample be  $M$ ,  $F$  ( $F < M$ ) attributes are randomly chosen from  $M$  to compose a random characteristic subspace  $X_i$ , and those as the split attribute sets of the present node of the decision tree. In the process of generating the RF model, the value of  $F$  remains unaltered;

Secondly, the node was split according to the optimal split attribute of each node selecting from the random feature subspace  $X_i$  by the decision tree generation algorithm;

Thirdly, every tree grows completely and has no pruning process. The corresponding decision tree  $h_i(D_i)$  is generated by each training set  $D_i$ ;

Fourthly, the FR model of  $\{h_1(D_1), h_2(D_2), \dots, h_i(D_i)\}$  was generated by combining all the generated decision trees. And the corresponding classification result of  $\{C_1(X), C_2(X), \dots, C_K(X)\}$  is obtained by using testing of each decision tree  $h_i(D_i)$  with test set sample  $X$ ;

Finally, according to the classification results of  $K$  decision trees, the final classification results corresponding to the test set sample  $X$  was determined by classification results with large number of decision trees by voting method.

#### (4) Dividing levels:

According to the above steps, the landslide susceptibility of Zhaoping County is divided into 5 levels (Fig. 4c).

### 3.4. Weighted random forest based on particle swarm optimization algorithm (PSO-RF)

In order to further compare the performance of different models in the evaluation of the susceptibility of the landslide, the parameters of the weighted FR are optimized by the PSO algorithm, and the main steps are as Table 4:

**Table 4** The main steps of the PSO-FR model

#### (1) Initialization:

The initial parameters of the PSO-FR model are set, including number of decision tree  $R$ , pruning threshold  $\varepsilon$ , number of predicted test samples  $X$ , and initial value of random attributes  $m$ .

#### (2) Sampling:




---

Using the Bootstrap algorithm,  $R$  training sets are randomly produced, and  $X$  pre-test samples are selected in each training set.

---

**(3) Generating decision tree:**

---

A total of  $R$  decision trees is generated by using the rest of the samples of each training set. In the process of generating decision trees,  $m$  attributes are selected from all attributes as the decision attributes of the present node before each attribute is selected.

---

**(4) Determination:**

---

When the number of samples included in the node is less than the threshold  $\epsilon$ , the node is taken as the leaf node, and the mode of the target attributes is returned as the classification result of the decision tree.

---

**(5) Setting up the PSO-SVM model:**

---

When all decision trees are produced, each decision tree is pre-tested and its weights are calculated by using the following formula:

$$w_r = \frac{X_{correct,r}}{X}, r = 1, 2, \dots, R \quad (7)$$

where  $X_{correct,r}$  is the classified correct number of samples of  $r$  decision trees, and  $X$  is the number of pre-tested samples.

---

**(6) Calculation of the classification results:**

---

The classification results of the model are calculated by the following formula:

$$f_{WRF}(x) = \arg \max_{i=1,2,\dots,C} \left\{ \sum_{r \in R, f_{tree,r}(x)=i} w_r \right\} \quad (8)$$


---

**(7) Optimization:**

---

Taking the classification results as the fitness values, the PSO algorithm is applied to optimize the parameters of formula (6) iteratively and determined the parameters of the final RF model.

---

**(8) Running**

---

Finally, the optimized parameters are input into the model, and the output results of the model are obtained. According to the results, the susceptibility of landslide is divided into five levels (Fig 4d).

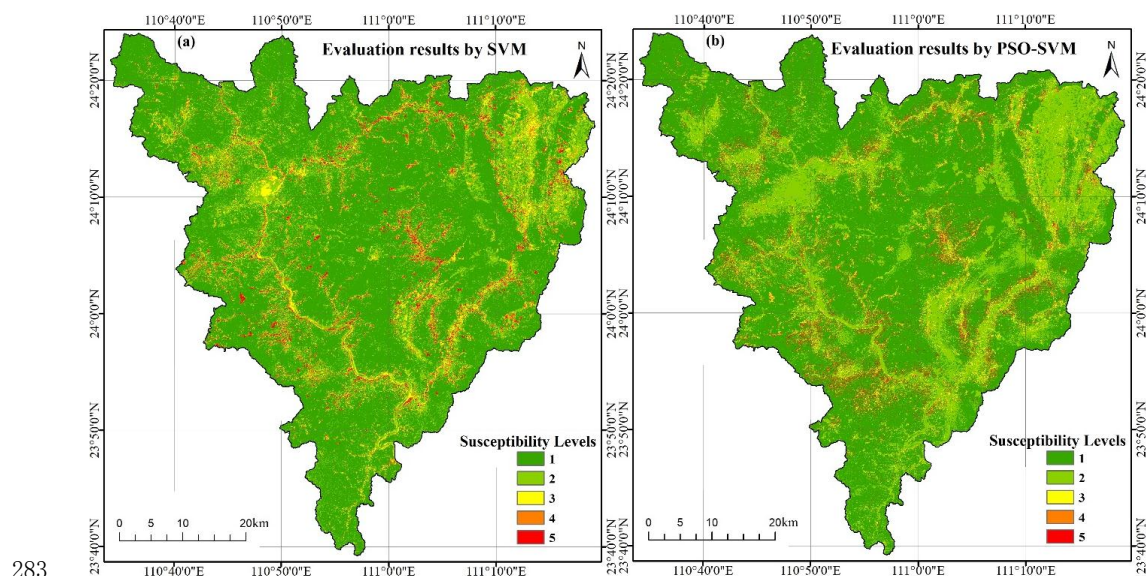
---



## 277 4. Results and discussions

### 278 4.1. Evaluation results

279 The 3,581,859 grids of Zhaoping County were input into the aboved four ML models, and  
 280 homologous output values were obtained. According to these output results, the landslide  
 281 susceptibility of Zhaoping County was divided into five levels: very low, low, moderate, high and  
 282 very high, as shown in Fig. 4.



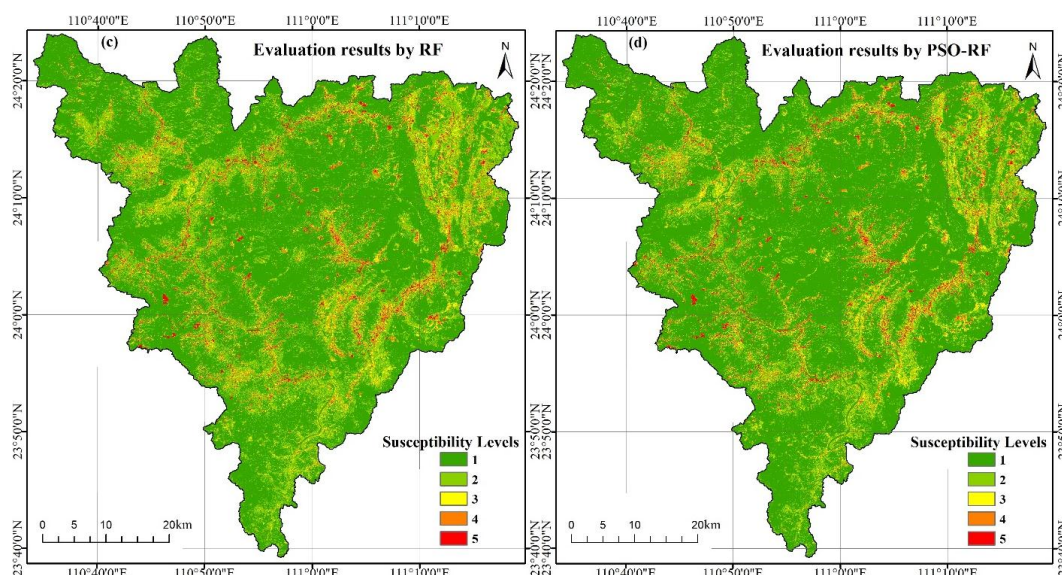


**Fig. 4.** Evaluation results of landslide susceptibility for four ML models in Zhaoping County [1-extremely low, 2-low, 3-middle, 4-high, 5-extremely high; (a) SVM; (b) PSO-SVM; (c) RF; (d) PSO-RF]

Figure 4 shows that the extremely high susceptibility levels for landslide is mainly distributed in the clastic rock areas along the Guijiang River and its tributaries, and the closer the river bank, the higher its susceptibility index. Here the geological structure is complex, where multi-period tectonic movement makes the joints and fractures of rock mass develop, the weathering of rock is serious, and water erosion is strong. Under the action of precipitation, especially heavy precipitation, as well as undermining and erosion of river water, clastic rocks are easy to form landslide disaster.

Simultaneously, Fig. 4 indicates that the high susceptibility levels for landslide is mainly distributed in the surrounding towns and trunk lines built near the mountains or the Guijiang River. Here the geological structure is relatively complex, the stability of rock is poor and weathering is strong, which supplies adequate material basis for the development of landslide



298 disaster. Simultaneously, the NDVI map of these regions indicate that the vegetation coverage in  
299 these regions is low, which indirectly reflects the frequent human engineering activities in the  
300 region, indicating that the human engineering construction strongly interferes with the geological  
301 ecological environment of the region and leads to the frequent occurrence of landslide. This also  
302 illustrates that the stability and bearing capacity of regional geological environment system  
303 should be fully considered in the construction of human engineering.

304 Figure 4 also indicates that the medium susceptibility levels for landslide is mainly  
305 distributed along the county roads, rural roads and residential areas, distributed in belts or  
306 surface-like distribution. The rock mass here is stable; the vegetation covers well, and is less  
307 disturbed by human activities.

308 The remaining areas are low and extremely low susceptibility levels for landslide, far away  
309 from the Guijiang River and its tributaries, with high vegetation coverage and less human  
310 engineering activities.

## 311 **4.2. Evaluation accuracy and validation analysis**

312 Evaluation accuracy and validation analysis is an essential component in landslide  
313 susceptibility prediction and evaluation to attest the availability and scientific significance of the  
314 adopted method (Fratini et al., 2010). Many research papers confirmed that the area under curve  
315 (AUC) of the receiver operating characteristic (ROC) curve was an effective method for the  
316 precision inspection of the prediction model, and was widely used in all subjects (Hanley and Mc  
317 Neil, 1983; Fawcett, 2005; Rossi et al., 2010; Pham et al., 2016; Tien Bui et al., 2016; Chen et al.,





2017; Lin et al., 2017; Hong et al., 2018; Ciurleo et al., 2019). Therefore, the AUC values of the ROC curves were used to evaluate the accuracy of landslide susceptibility in Zhaoping County for the ML methods, such as the SVM, PSO-SVM, RF, and PSO-RF model, as shown in Fig. 5.

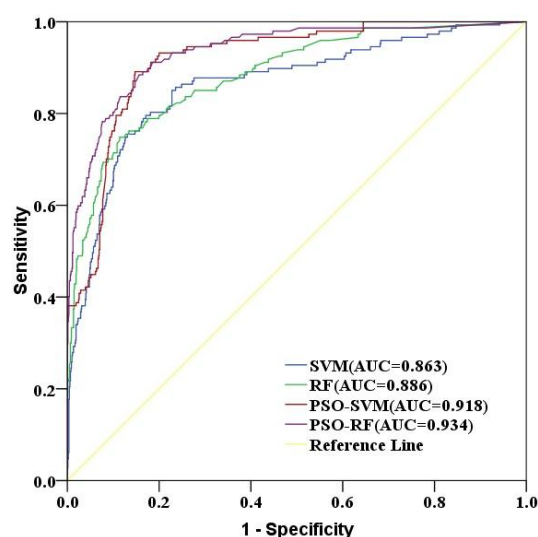


**Fig. 5.** ROC curves and AUC values of validation set for the PSO-RF, RF, PSO-SVM, and SVM model

Figure 5 indicates the ROC curves and the AUC values of the validation set for the PSO-RF, RF, PSO-SVM, and SVM models. The values of AUC are 0.934, 0.886, 0.918, 0.863, respectively, which indicate that the accuracy of the four ML methods in the evaluation and prediction of landslide susceptibility in Zhaoping County is higher than 86%. At the same time, the AUC values of the PSO-SVM and PSO-RF models (0.918 and 0.934) were higher than those of the traditional SVM and the RF (0.863 and 0.886), which indicated that the PSO algorithm can effectively optimize SVM and RF models, and the prediction accuracy of the optimized model is more than 91.5%. Such a result further revealed that the PSO-RF and PSO-SVM models have the stronger robustness and stable performance. Furthermore, the present study further testified that





332 PSO has strong global parameter search ability, and parameter adjustment is simple and easy to  
 333 implement, which confirmed that the PSO algorithm is successfully applied in landslide hazards  
 334 evaluation and prediction (Liu et al., 2012; Feng et al., 2017; Hoang and Tien Bui, 2018).

335 Figure 5 indicates that the performance of the RF and RF-PSO is better than the SVM and  
 336 PSO-SVM in evaluating the susceptibility of landslide because the values of AUC for RF (0.886)  
 337 and RF-PSO (0.934) are higher than the values of AUC for SVM (0.863) and PSO-SVM (0.918),  
 338 respectively, which confirmed that the generalization performance of the integrated learner is  
 339 superior to that of a single learner (Li et al., 2014; Zhang et al., 2018). At the same time, the  
 340 research further certified that the RF and PSO-RF models have advantages in dealing with high  
 341 dimensional features and geological big data, such as fast classification speed, strong anti-noise  
 342 ability, and avoiding over-fitting (Tien Bui et al., 2016). However, because of the sensitivity of  
 343 the RF and PSO-RF models to the proportion of landslide samples, it is necessary to carry out  
 344 sample screening before using RF and PSO-RF models to evaluate the susceptibility of landslide.

345 In order to further verify the accuracy of the four ML models, the ratio of grid number of  
 346 landslide points that fall into different susceptibility levels was counted, as shown in Table 5:

347 **Table 5** Percentages of landslide points falling into different susceptibility levels

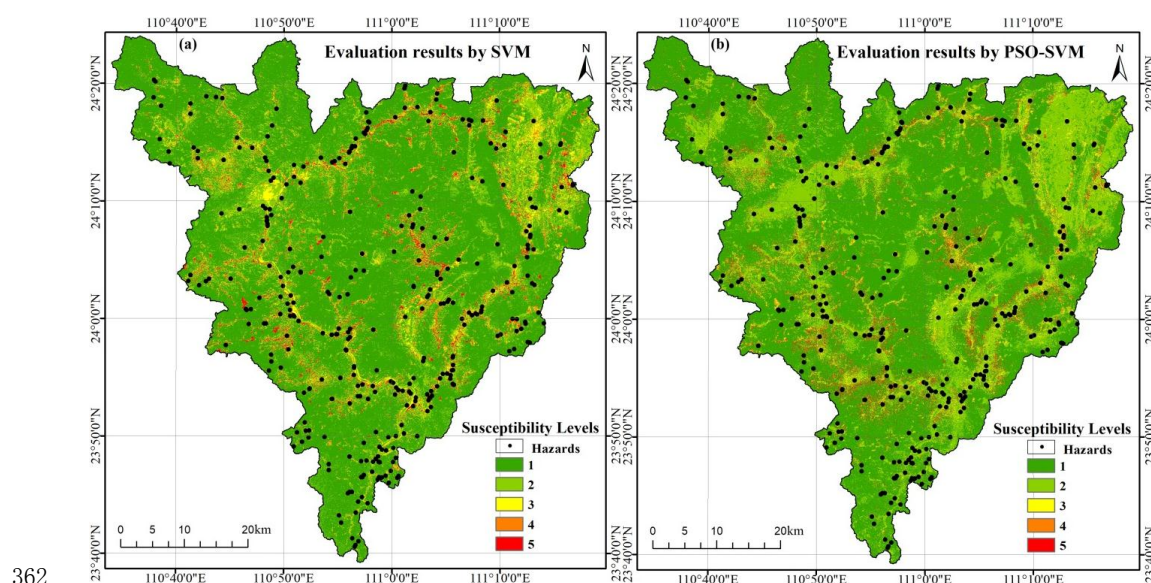
Susceptibility levels	SVM (%)	PSO-SVM (%)	RF (%)	PSO-RF (%)
Extremely high	0.1238	0.2030	0.1793	0.2306
High	0.0561	0.0609	0.0596	0.0845
Medium	0.0302	0.0232	0.0171	0.0117
Low	0.0124	0.0057	0.0077	0.0041
Extremely low	0.0010	0.0006	0.0008	0.0005

348 Table 5 indicates that the proportions of hazards points falling into extremely high and high  
 349 susceptibility regions are 0.2306% and 0.0845%, 0.2030% and 0.0609%, 0.1793% and 0.0596%,



and 0.1238% and 0.0561% for the PSO-FR, PSO-SVM, RF, and SVM models, respectively, which certified that the evaluation accuracy of four ML models in the extremely high and high prone regions from high to low are: PSO-RF, PSO-SVM, RF, and SVM. Simultaneously, Table 5 also indicates that the proportions of landslide points falling into low and extremely low susceptibility regions are 0.0041% and 0.0005%, 0.0057% and 0.0006%, 0.0077% and 0.0008%, and 0.0124% and 0.0010% for the PSO-FR, PSO-SVM, RF, and SVM models, respectively, which certified that the wrong accuracy of four ML models in the low and extremely low susceptibility regions from low to high are: PSO-RF, PSO-SVM, RF, and SVM.

In addition to the above two methods of verification, field investigation has been implemented by Guangxi Geological Survey Bureau in Zhaoping County. Simultaneously, the field investigation results were compared and analyzed with the evaluation results of four ML models, as shown in Fig. 6:



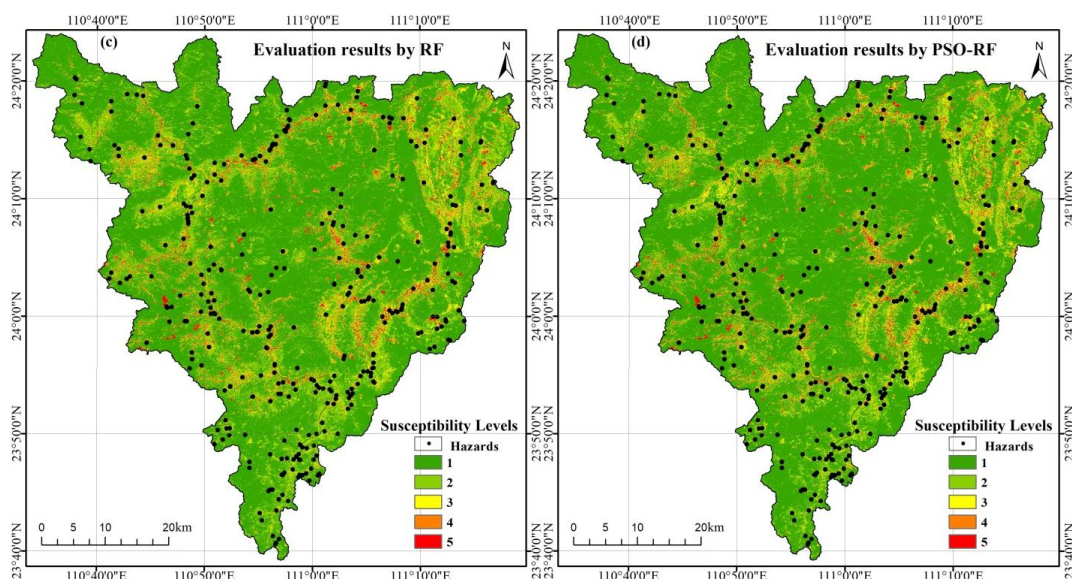


**Fig. 6.** Landslide susceptibility overlying maps of field survey and evaluation results for four ML models in Zhaoping County [1-extremely low, 2-low, 3-middle, 4-high, 5-extremely high; (a) SVM, (b) PSO-SVM, (c) RF, (d) PSO-RF]

Figure 6 indicates that the landslide susceptibility evaluation results of four ML models in Zhaoping County are in accord with the distribution of landslide points of field investigation, which further illustrates that the methods in evaluating landslide susceptibility in the present paper was reasonable and effective.

Overall, the ML models of the SVM, PSO-SVM, RF, and PSO-RF achieved excellent performance in predicting and evaluating the susceptibility levels of landslide in this study.



## 373 5. Conclusions

374 The improvement of performance for landslide susceptibility models is still the focus of  
375 widespread concern in the disaster research community, because the capability of the models is  
376 dominated by the method adopted (Tien Bui et al., 2016); though ML methods have been  
377 validated efficient in terms of prediction and assessment performance (Pham et al., 2016).  
378 Therefore, four widely used ML models such as SVM, PSO-SVM, RF, and PSO-RF were  
379 investigated to predict and evaluate the susceptibility levels of landslide for Zhaoping County in  
380 Guangxi of southern China.

381 Analysis and comparison of the results denoted that all four ML models performed well for  
382 the landslide susceptibility evaluation and prediction as the AUC values of ROC curves are all  
383 greater than 86%. Thereinto, it has been shown that the PSO-RF model (93.4%) has the highest  
384 accuracy in comparison to other landslide models, followed by the PSO-SVM model (91.8%), the  
385 RF model (88.6%), and the SVM model (86.3%). Moreover, the results also showed that the PSO  
386 algorithm has a good effect on SVM and FR models. In addition, our results also revealed that the  
387 PSO-RF and PSO-SVM landslide models have the strong robustness and stable performance, and  
388 those two models are prospective methods that could be applied to landslide susceptibility  
389 evaluation in similar natural geological and ecological environment background regions.

390 At the same time, the results described in the present study proved that the prediction results  
391 of four ML models are consistent with the field survey results by comparing Fig. 4 and Fig. 6,  
392 which verified the validity of the four ML models again. This also proved that the ML models  
393 have excellent performance in evaluating and predicting the occurrence of landslide. Furthermore,



394 the results can provide informational service and decision support for landslide early warning,  
395 land use planning and environmental management for local government departments.

396 In addition, our study found that the 10 disaster-related factors selected in this paper can fully  
397 reflect the natural geological and ecological environment characteristics of the study area, and  
398 have a great correlation to the occurrence of landslide disasters. Simultaneously our study also  
399 found that the selection of training samples will affect the susceptibility evaluation results during  
400 the process of landslide susceptibility evaluation using four ML methods. It is worth mentioning  
401 that there is a great difference between the extremely low and extremely high susceptibility  
402 regions for the evaluation results of RF and PSO-RF model, and the occurrences of the extremely  
403 low prone regions is almost 0. However, regions where landslide hazards have not occurred do  
404 not mean that landslide will not occur, so future investigations should pay more attention to  
405 over-fitting in evaluating and predicting the susceptibility of landslide for the RF and PSO-RF  
406 models.



407 **Code availability**

408 The following program is used to optimize parameters in SVM, PSO-SVM, RF, and PSO-RF,  
409 and further use the optimized parameters to set up training models of SVM, PSO-SVM, RF, and  
410 PSO-RF.

411 Name of code: gaSVMcgForClass.m, SVMcgForClass.m, main.py

412 Developer and contact address: Kong Chunfang, Wang Junzuo

413 Telephone number and E-mail: +8618602766895, kongcf@cug.edu.cn

414 Year first available: YES

415 Hardware required: CPU-i5, MEMORY-4G

416 Software required: WIN10, matlab R2018a, Spyder

417 Program language: M language, Python

418 Program size: 9.35k

419 The code can be accessed using the following link: <https://github.com/kongcf/mycode.git>



420 **Data availability**

421 All data used during the study are available in 4TU Research Data repository and can be  
422 accessed through this doi link: <https://doi.org/10.4121/12857417.v1>



423 **Author contributions**

424 All the authors made significant contributions to the work. Kong C.F. and Xu K. designed  
425 the research, analyzed the results, and accomplished the validation work; Wang J.Z. completed  
426 the data acquisition, analysis or interpretation; Wu C.L. and Liu G. provided advice for the  
427 revision of the paper. All authors give their final approval of the manuscript version to be  
428 submitted and any revised version of it.





429 **Competing interests**

430 The authors declare that they have no conflict of interest.



## 431 **Acknowledgments**

432       The authors would like to thank the Guangxi Geological Survey Bureau for providing the  
433 various data sets used in this paper. This work has been supported by the National Natural  
434 Science Foundation of China (No: 41201193); Guizhou Science and Technology Planning Project:  
435 Research and Application of Three-dimensional Prediction System for Gold Deposit in Southwest  
436 Guizhou Based on Geological Big Data ([2020]4Y039); Research and Development of Big Data  
437 Management and Intelligent Processing System for Manganese Ore Exploration ([2017]2951);  
438 Open fund project of National-Local Joint Engineering Laboratory on Digital Preservation and  
439 Innovative Technologies for the Culture of Traditional Villages and Towns (CTCZ19K01), and  
440 Open research project of key laboratory of Tectonics and Petroleum Resources (China University  
441 of Geosciences), Ministry of Education (No: TPR-2019-11). The authors would like to thank the  
442 anonymous reviewers for providing valuable comments on the manuscript.



## References

- Ada, M., and San, B. T.: Comparison of machine-learning techniques for landslide susceptibility mapping using two-level random sampling (2LRS) in Alakir catchment area, Antalya, Turkey. *Nat. Hazard.*, 90, 237–263, 2018.
- Aditian, A., Kubota, T., and Shinohara, Y.: Comparison of GIS-based landslide susceptibility models using frequency ratio, logistic regression, and artificial neural network in a tertiary region of Ambon, Indonesia. *Geomorphology*, 318, 101–111, 2018.
- Aktas, H. and San, B.T.: Landslide susceptibility mapping using an automatic sampling algorithm based on two level random sampling. *Comput. Geosci.*, 133, 1–17, 2019.
- Breiman, L.: Random forests. *Machine Learning*, 45(1), 5–32, 2001.
- Chen, Q., Liu, G., Ma, X., Zhang, J., and Zhang, X.: Conditional multiple-point geostatistical simulation for unevenly distributed sample data. *Stoch. Env. Res. Risk A.*, 33, 973–987, 2019.
- Chen, W., Xie, X., Wang, J., Pradhan, B., Hong, H., Bui, D. T., Duan, Z., and Ma, J.: A comparative study of logistic model tree, random forest, and classification and regression tree models for spatial prediction of landslide susceptibility. *Catena*, 151, 147–160, 2017.
- Choi, J., Oh, H. J., Lee, H. J., Lee, C., and Lee, S.: Combining landslide susceptibility maps obtained from frequency ratio, logistic regression, and artificial neural network models using ASTER images and GIS. *Eng. Geol.*, 124, 12–23, 2012.
- Ciurleo, M., Mandaglio, M. C., and Moraci, N.: Landslide susceptibility assessment by TRIGRS in a frequently affected shallow instability area. *Landslides*, 16, 175–188, 2019.



- 464 Conforti, M., Pascale, S., Robustelli, G., and Sdao, F.: Evaluation of prediction capability of the  
 465 artificial neural networks for mapping landslide susceptibility in the Turbolo River  
 466 catchment (northern Calabria, Italy). *Catena*, 113, 236–250, 2014.
- 467 Cortes, C. and Vapnik, V.: Support vector networks. *Mach. Learn.*, 20(3), 273–297, 1995.
- 468 Fawcett, T.: An introduction to ROC analysis. *Pattern Recogn. Lett.*, 27(8), 861–874, 2005.
- 469 Fang, Z., Wang, Y., Peng, L., and Hong, H.: Integration of convolutional neural network and  
 470 conventional machine learning classifiers for landslide susceptibility mapping, *Comput.*  
 471 *Geosci.*, doi: <https://doi.org/10.1016/j.cageo.2020.104470>, 2020.
- 472 Feng, F., Wu, X., Niu, R., Xu, S., and Yu, X.: Landslide susceptibility assessment based on  
 473 PSO-BP neural network, *Sci. Surv. Mapp.*, 42(10), 170–175, 2017.
- 474 Frattini, P., Crosta, G., and Carrara, A.: Techniques for evaluating the performance of landslide  
 475 susceptibility models, *Eng. Geol.*, 111(1), 62–72, 2010.
- 476 Hanley, J. A. and Mc Neil, B. J.: A method of comparing the areas under receiver operating  
 477 characteristic curves derived from the same cases. *Radiology*, 148(3), 839–843, 1983.
- 478 Hoang, N. D. and Tien Bui, D.: Spatial prediction of rainfall-induced shallow landslides using  
 479 gene expression programming integrated with GIS: A case study in Vietnam. *Nat. Hazard.*,  
 480 92(3), 1871–1887, 2018.
- 481 Hong, H., Pradhan, B., Xu, C., and Tien Bui, D.: Spatial prediction of landslide hazard at the  
 482 Yihuang area (China) using two-class kernel logistic regression, alternating decision tree and  
 483 support vector machines. *Catena*, 133, 266–281, 2015.
- 484 Hong, H., Liu, J., Tien Bui D., Pradhan, B., Acharya, T. D., Pham, B. T., Zhu, A., Chen, W., and



- 485 Ahma, B. B.: Landslide susceptibility mapping using J48 decision tree with Adaboost,  
 486 bagging and rotation forest ensembles in the Guangchang area (China). *Catena*, 163, 399–  
 487 413, 2018.
- 488 Huang, Y. and Zhao, L.: Review on landslide susceptibility mapping using support vector  
 489 machines. *Catena*, 165, 520–529, 2018.
- 490 Kavzoglu, T., Sahin, E. K., and Colkesen, I.: Landslide susceptibility mapping using GIS based  
 491 multi-criteria decision analysis, support vector machines, and logistic regression. *Landslides*,  
 492 11, 425–439, 2014.
- 493 Khosravi, K., Pham, B. T., Chapi, K., Shirzadi, A., Shahabi, H., Revhaug, I., Prakash, I., and Bui,  
 494 D. T.: A comparative assessment of decision trees algorithms for flash flood susceptibility  
 495 modeling at Haraz watershed, northern Iran. *Sci. Total. Environ.*, 627, 744–755, 2018.
- 496 Kumar, D., Thakur, M., Dubey, C. S., and Shukla, D. P.: Landslide susceptibility mapping &  
 497 prediction using support vector machine for Mandakini River Basin, Garhwal Himalaya,  
 498 India. *Geomorphology*, 295, 115–125, 2017.
- 499 Li, T., Tian, Y., Wu, L., and Liu, L.: Landslide susceptibility mapping using random forest. *Geogr.*  
 500 *Geo-inf. Sci.*, 30(6), 25–30, 2014.
- 501 Lin, L., Lin, Q., and Wang, Y.: Landslide susceptibility mapping on a global scale using the  
 502 method of logistic regression. *Nat. Hazard. Earth Sys.*, 17(8), 1411–1424, 2017.
- 503 Liu, Y., Yang, X., Fu, N., and Wang, Y.: Method of particle swarm optimization neural network  
 504 on geological hazards comprehensive evaluation and its application. *J. Seismol. Res.*, 35(4),  
 505 571–577, 2012.



- 506 Marjanović, M., Kovačević, M., Bajat, B., and Voženilek, V.: Landslide susceptibility assessment  
 507 using SVM machine learning algorithm. *Eng. Geol.*, 123, 225–234, 2011.
- 508 Murillo-García, F. G. and Alcántara-Ayala, I.: Landslide Susceptibility Analysis and Mapping  
 509 Using Statistical Multivariate Techniques: Pahuatlán, Puebla, Mexico, Recent Advances in  
 510 Modeling Landslides and Debris Flows. Springer, 179–194, 2015.
- 511 Peng, L., Niu, R., Huang, B., Wu, X., Zhao, Y., and Ye, R.: Landslide susceptibility mapping  
 512 based on rough set theory and support vector machines: a case of the Three Gorges area,  
 513 China. *Geomorphology*, 204(1), 287–301, 2014.
- 514 Pham, B. T., Pradhan, B., Tien Bui, D., Prakash, I., and Dholakia, M. B.: A comparative study of  
 515 different machine learning methods for landslide susceptibility assessment: a case study of  
 516 Uttarakhand area (India). *Environ. Modell. Softw.*, 84, 240–250, 2016.
- 517 Pham, B. T., Tien Bui, D., Pourghasemi, H. R., Indra, P., and Dholakia, M. B.: Landslide  
 518 susceptibility assessment in the Uttarakhand area (India) using GIS: A comparison study of  
 519 prediction capability of naïve bayes, multilayer perceptron neural networks, and functional  
 520 trees methods. *Theor. Appl. Climatol.*, 122, 1–19, 2015.
- 521 Pourghasemi, H. R., Jirandeh, A. G., Pradhan, B., Xu, C., and Gokceoglu, C.: Landslide  
 522 susceptibility mapping using support vector machine and GIS at the Golestan Province, Iran.  
 523 *J. Earth Syst. Sci.*, 2, 349–369, 2013.
- 524 Pourghasemi, H. R., Mohammady, M., and Pradhan, B.: Landslide susceptibility mapping using  
 525 index of entropy and conditional probability models in GIS: Safarood Basin, Iran. *Catena*,  
 526 97, 71–84, 2012.



- 527 Pradhan, B.: A comparative study on the predictive ability of the decision tree, support vector  
 528 machine and neuro-fuzzy models in landslide susceptibility mapping using GIS. *Comput.*  
 529 *Geosci.*, 51(2), 350–365, 2013.
- 530 Rossi, M., Guzzetti, F., Reichenbach, P., Mondini, A. C., and Peruccacci, S.: Optimal landslide  
 531 susceptibility zonation based on multiple forecasts. *Geomorphology*, 114(3), 129–142, 2010.
- 532 San, B.T.: An evaluation of SVM using polygon-based random sampling in landslide  
 533 susceptibility mapping: The Candir catchment area (western Antalya, Turkey). *Int. J. Appl.*  
 534 *Earth Obs. Geoinf.*, 26, 399–412, 2014.
- 535 Sevgen, E., Kocaman, S., Nefeslioglu, H. A., and Gokceoglu, C.: A novel performance  
 536 assessment approach using photogrammetric techniques for landslide susceptibility mapping  
 537 with logistic regression, ANN and random forest. *Sensors*, 19, 3940, 2019.
- 538 Song, Y., Gong, J., Gao, S., Wang, D., Cui, T., Li, Y., and Wei, B.: Susceptibility assessment of  
 539 earthquake-induced landslides using Bayesian network: a case study in Beichuan, China.  
 540 *Comput. Geosci.*, 42, 189–199, 2012.
- 541 Tax, D. and Duin, E.: Support vector domain description. *Pattern Recogn. Lett.*, 20, 1191–1199,  
 542 1999.
- 543 Tien Bui, D., Pradhan, B., Lofman, O., and Revhaug, I.: Landslide susceptibility assessment in  
 544 Vietnam using support vector machines, decision tree, and Naïve Bayes models. *Math.*  
 545 *Problems Eng.*, 1–26, 2012.
- 546 Tien Bui, D., Tuan, T. A., Klempe, H., Pradhan, B., and Revhaug, I.: Spatial prediction models  
 547 for shallow landslide hazards: a comparative assessment of the efficacy of support vector



- 548 machines, artificial neural networks, kernel logistic regression, and logistic model tree.
- 549 Landslides, 13(2), 361–378, 2016.
- 550 Trigila, A., Iadanza, C., Esposito, C., and Scarascia-Mugnozza, G.: Comparison of logistic
- 551 regression and random forests techniques for shallow landslide susceptibility assessment in
- 552 Giampileri (NE Sicily, Italy). *Geomorphology*, 249, 119–136, 2015.
- 553 Tsai, F., Lai, J., Chen, W., and Lin, T.: Analysis of topographic and vegetative factors with data
- 554 mining for landslide verification. *Ecol. Eng.*, 61, 669–677, 2013.
- 555 Vapnik, V. N.: *The Nature of Statistical Learning Theory*. Springer, New York: John Wiley and
- 556 Sons., 316, 1995.
- 557 Wang, N., Guo, Y., Liu, T., and Zhu, Q.: Assessment of landslide susceptibility based on
- 558 SVM-LR model: A case study of Lintong district. *Sci. Technol. Eng.*, 19(30), 62–69, 2019.
- 559 Xia, H., Yin, K., Liang, X., and Ma, F.: Landslide susceptibility assessment based on SVM-ANN
- 560 Models: a case study for Wushan County in the Three Gorges Reservoir. *Chinese J. Geol.*
- 561 *Hazard Contr.*, 29(5), 13–19, 2018.
- 562 Xu, K., Guo, Q., Li, Z., Xiao, J., Qin, Y., Chen, D., and Kong, C.: Landslide susceptibility
- 563 evaluation based on BPNN and GIS: a case of Guojiaba in the Three Gorges Reservoir Area.
- 564 *Int. J. Geogr. Inf. Sci.*, 29(7), 1111–1124, 2015.
- 565 Youssef, A. M., Pourghasemi, H. R., Pourtaghi, Z. S., and Al-Katheeri, M. M.: Landslide
- 566 susceptibility mapping using random forest, boosted regression tree, classification and
- 567 regression tree, and general linear models and comparison of their performance at Wadi
- 568 Tayyah Basin, Asir Region, Saudi Arabia. *Landslides*, 13(5), 839–856, 2016.





- 569 Zare, M., Pourghasemi, H. R., Vafakhah, M., and Pradhan, B.: Landslide susceptibility mapping  
 570 at Vaz Watershed (Iran) using an artificial neural network model: a comparison between  
 571 multilayer perceptron (MLP) and radial basic function (RBF) algorithms. Arab. J. Geosci.,  
 572 6(8), 2873–2888, 2013.
- 573 Zhang, L., Shi, S., and Liu, Q.: Spatial-temporal distribution characteristics and genetic analysis  
 574 of geological disasters in Guangxi. Guangxi Water Resour. Hydropower Eng., 6, 64–67,  
 575 2016.
- 576 Zhang, X., Wang, M., Cao, Y., Liu, K., and Hong, C.: Comparison of three typical machine  
 577 learning methods in susceptibility assessment of disasters. J. Safety Sci. Technol., 14(7), 79–  
 578 85, 2018.
- 579 Zhang, T., Han, L., Zhang, H., Zhao, Y., and Zhao, L.: GIS-based landslide susceptibility  
 580 mapping using hybrid integration approaches of fractal dimension with index of entropy and  
 581 support vector machine. J. MT Sci., 16(6), 1275–1288, 2019.
- 582 Zhou, C., Yin, K., Cao, Y., Ahmed, B., Li, Y., Catani, F., and Pourghasemi, H.R.: Landslide  
 583 susceptibility modeling applying machine learning methods: A case study from Longju in  
 584 the Three Gorges Reservoir area, China. Comput. Geosci., 112, 23–37, 2018.